

**Flexible Macroscopic Models for Dense-Fluid Shockwaves:
Partitioning Heat and Work; Delaying Stress and Heat Flux;
Two-Temperature Thermal Relaxation**

Wm. G. Hoover and C. G. Hoover

Ruby Valley Research Institute

Highway Contract 60, Box 598

Ruby Valley, Nevada 89833

and Francisco J. Uribe

Department of Physics

Universidad Autónoma Metropolitana

Mexico City, Mexico 09340

(Dated: February 26, 2018)

Abstract

Macroscopic models which distinguish the longitudinal and transverse temperatures can provide improved descriptions of the microscopic shock structures as revealed by molecular dynamics simulations. Additionally, we can include three relaxation times in the models, two based on Maxwell's viscoelasticity and its Cattaneo-equation analog for heat flow, and a third thermal, based on the Krook-Boltzmann equation. This approach can replicate the observed lags of stress (which lags behind the strain rate) and heat flux (which lags behind the temperature gradient), as well as the eventual equilibration of the two temperatures. For profile stability the time lags cannot be too large. By partitioning the longitudinal and transverse contributions of work and heat and including a tensor heat conductivity and bulk viscosity, all the qualitative microscopic features of strong simple-fluid shockwave structures can be reproduced.

PACS numbers:

Keywords:

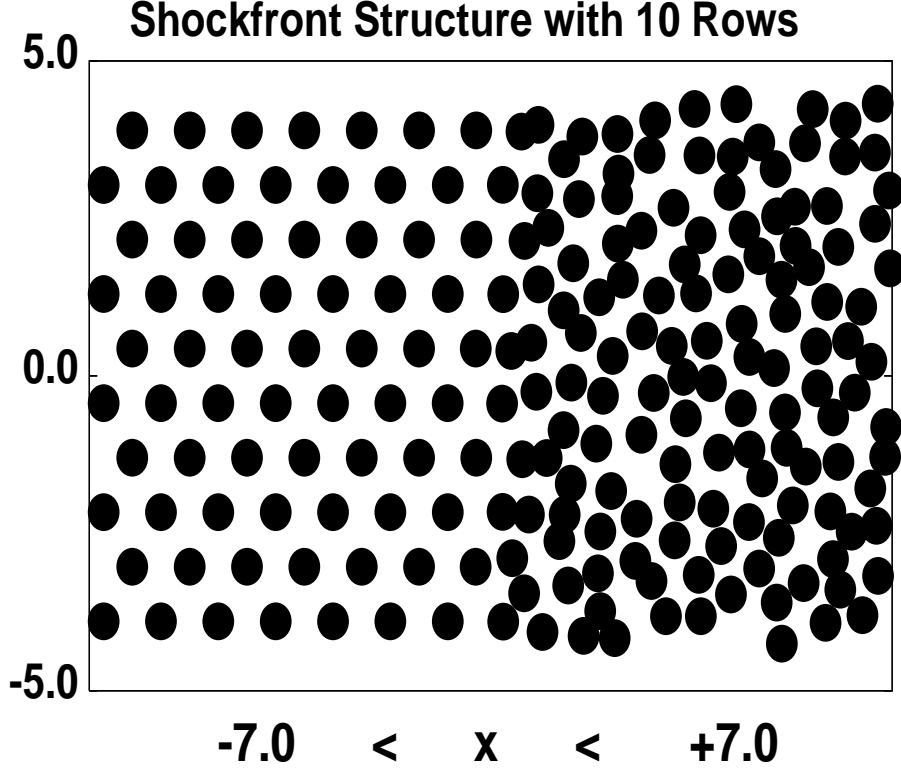


FIG. 1: The steady flow shown here pictures cold material, moving to the right at speed u_s and decelerated by slower hot fluid, moving to the right at speed $u_s - u_p$, with u_s and u_p chosen to fix the shockwave location in space, $u_{wave} = 0$. An alternative way to generate such shockwaves is shown in Figure 2.

I. INTRODUCTION: PROPERTIES OF DENSE-FLUID SHOCKWAVES

Stationary shockwaves provide the simplest possible opportunity for the study of highly nonlinear transport in dense fluids. In the shock-centered steady-state coordinate frame, the nonequilibrium shock process converts an incoming steady stream of “cold” material into an outgoing stream of “hot” fluid. See Figure 1. Shockwave gradients can be huge, with strainrates in the terahertz range and correspondingly large pressure and temperature gradients, 10^{15} atmospheres/centimeter and 10^{12} kelvins/centimeter¹. Despite the wildly irreversible nature of such a nonequilibrium conversion, so long as the shock is stationary the overall internal energy change, $E_H - E_C$, can be expressed in terms of the equilibrium pressures and volumes of the incoming and outgoing streams of fluid:

$$\Delta E = E_H - E_C = (P_H + P_C)(V_C - V_H)/2 .$$

In the steady-state coordinate frame centered on the shockwave (Figure 1), the incoming cold material, moving at the shock velocity u_s , is decelerated to $u_s - u_p$ by the shockfront, where u_p is the “particle”, or “piston”, velocity.

The Hugoniot relation for the energy change ΔE , just given, can be derived by eliminating the two velocities u_s and u_p from the three conservation equations for mass, momentum, and energy². An alternative shock-creation mechanism, quite practical for computer simulation, uses the symmetric collision of two blocks of cold fluid. For problems with a nonzero initial pressure confining pistons are required. In either case the two blocks approach each other with velocities $\pm u_p$, and generate two mirror-image shockwaves identical in structure to those obtained with steady-state boundary conditions. See again Figure 1, as well as Figure 2, for the geometries of these two methods for generating shockwaves.

Over the last forty years a wide variety of atomistic shockwave simulations, based on molecular dynamics, have been carried out³⁻¹⁰. These particle-based simulations established three interesting facts which simplify numerical treatments of shockwaves. First fact: the *boundary conditions* enclosing the shockwave can be implemented easily because they are simply equilibrium states when viewed in a moving coordinate system. See again Figures 1 and 2. Second fact: shockwave thicknesses are indeed only a few mean free paths^{4,5,11}, as predicted for gases by numerical solutions of the Boltzmann equation¹²⁻¹⁷. The small scale of shockwaves makes molecular dynamics simulations relatively simple to carry out. Third fact: one-dimensional shockwaves are stable⁷, as shown in Figure 3. Stability means that it is sensible to measure and compute shockwave profiles in which density, velocity, and energy are all expressed as functions of a single longitudinal coordinate, here chosen to define the x axis.

In addition to these simplifying facts there are three more facts which complicate rather than simplify numerical treatments. They deserve more discussion and form the heart of the present work: fourth fact: temperature within the shockwave is a *tensor*, with different longitudinal and transverse values. Mott-Smith predicted the details of this complication for gases¹³, by using an approximate bimodal velocity distribution (a spatially-varying linear combination of the cold and hot Maxwellian distributions). We discuss the meaning of “temperature” in the following Section II^{7-9,12-14,18}.

A fifth fact, discovered in the course of comparisons of atomistic simulations with continuum predictions, is that the nonlocality of atomistic interactions introduces an essential

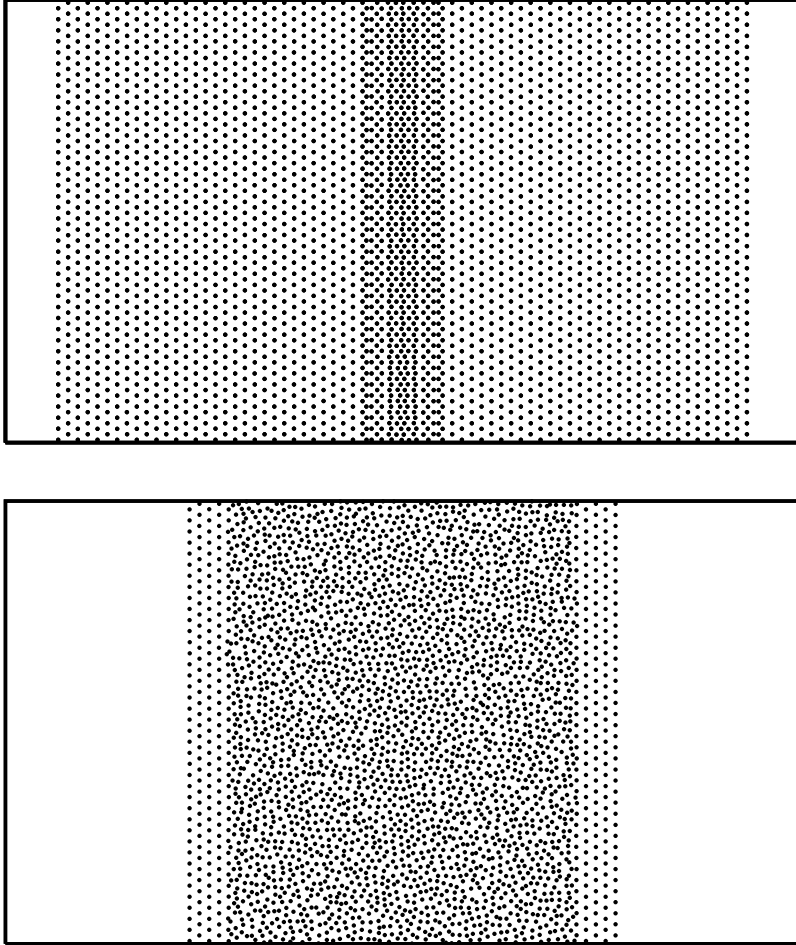


FIG. 2: Here two identical blocks of zero-pressure material at $\pm u_p$ have collided with sufficient velocity to compress the fluid to twice the initial density. The two shockwaves at the interface between the moving cold material and the stationary hot fluid are separating at velocities $\pm(u_s - u_p)$. The forces between particles, here and in Figures 1, 3, and 4, are short-ranged repulsive forces derived from the pair potential $\phi = (10/\pi)(1 - r)^3$.

dependence of spatial averages on the averaging algorithm itself. Any continuum treatment which aims to describe two- or three-dimensional phenomena must come to grips with an appropriate choice of averaging algorithm. Lucy's one-, two-, and three-dimensional weighting functions used in smooth particle applied mechanics¹⁹⁻²¹ provide a particularly appealing

solution to the problem. Averaging is addressed in Section III.

Last, a sixth fact, discovered more recently, is that relaxation and lag are characteristic of shockwaves. Strong shockwaves display cause-and-effect relaxation, with the shear stress, $\sigma = (P_{yy} - P_{xx})/2$, responding to the strain rate $\dot{\epsilon} = (du/dx)$ and the heat flux Q_x responding to the temperature gradient ∇T only after noticeable delays. These observed delay times are of the order of the particle-particle collision time⁹. Lag, relaxation, and delay are addressed in Section IV.

Existing models for shockwave structure, such as the linear-transport Navier-Stokes equations^{11,22} or the nonlinear-transport Burnett equations^{10,15-17,23}, need to be improved to take these recent shock-structure observations into account. Delay has to be included in the models and temperature needs to have its longitudinal and transverse components treated separately. The present work is devoted to developing and exploring a comprehensive description of shock dynamics and developing the numerical techniques necessary to implement the new findings into continuum simulations.

Following these discussions of thermal anisotropy, spatial nonlocality, and relaxation, we introduce a well-posed continuum model incorporating all these ideas and illustrate a numerical method for solving particular special cases in Section V. Section VI contains a summary of our results and an assessment of the prospects for future progress.

II. KINETIC TEMPERATURE AND ITS MEASUREMENT

Gibbs and Boltzmann related microscopic mechanics to macroscopic thermodynamics by showing that an ideal-gas thermometer¹⁸ satisfied the Zeroth law of thermodynamics²⁴. Two systems at thermal equilibrium with a Maxwell-Boltzmann ideal gas at the kinetic temperature

$$T_{gas} = T_{eq} \equiv \langle p_x^2/mk \rangle = \langle p_y^2/mk \rangle = \langle p_z^2/mk \rangle ,$$

are necessarily in thermal equilibrium with each other. Thus the ideal gas is a reliable thermometer and can be used to measure temperature in other gases, or in liquids, or in solids. Consider applying the ideal-gas definition of temperature to a steady, but nonequilibrium, shockwave. Then there are substantial coordinate-dependent disparities between the longitudinal and transverse kinetic temperatures,

$$\langle p_x^2/mk \rangle = T_{xx} ; \langle p_y^2/mk \rangle = T_{yy} .$$

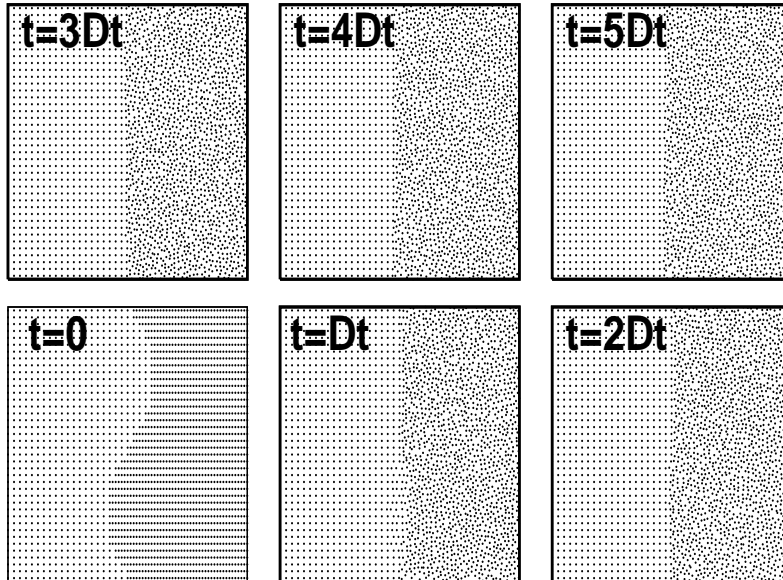


FIG. 3: Six snapshots, equally spaced in time, showing the underdamped oscillation of a sinusoidal shockwave. The hot shocked fluid is at twice the density of the cold unshocked material.

These kinetic temperatures are velocity fluctuations about the local mean velocity so that in the comoving measurement frame the mean values of the momenta vanish:

$$u(x) = \langle \dot{x} \rangle ; p_x \equiv m(\dot{x} - \langle \dot{x} \rangle) = m(\dot{x} - u(x)) ; \langle p_x \rangle = \langle p_y \rangle = 0 .$$

The kinetic definitions for the nonequilibrium longitudinal and transverse temperatures arise naturally if one imagines “measuring” them, for particular degrees of freedom, by putting the nonequilibrium fluid into diagnostic contact with a comoving ideal-gas thermometer¹⁸. Such a thermometer is best thought of as a tiny sample of equilibrated gas, with the gas made up of very many very small hard particles. These thermometric particles undergo impulsive collisions with selected system degrees of freedom. If the ideal-gas particles are very small the temperature measurement doesn’t change the dynamical state of the nonequilibrium fluid¹⁸. The ideal-gas nature of the thermometer makes it possible to analyze the collisions from the two-body standpoint of the Boltzmann equation. Hard-disk or hard-sphere interactions between the thermometer and the system change, on average, the total kinetic energy of a system particle if it deviates from the thermometer’s temperature. If the thermometer particles are instead pictured as parallel hard cubes (parallel squares in

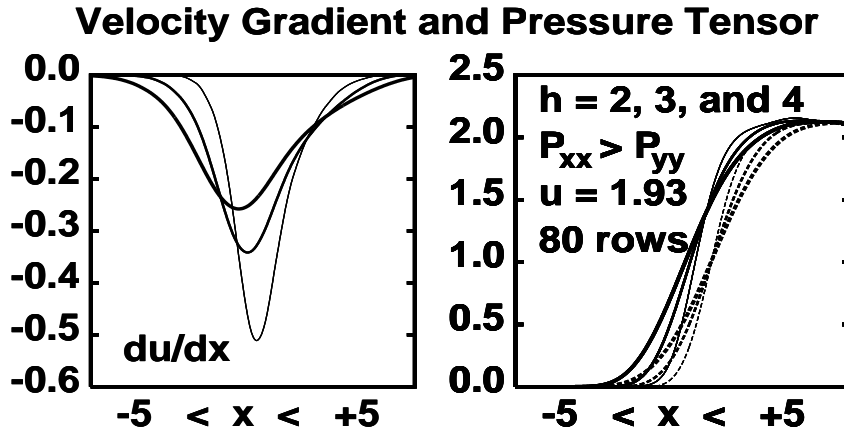


FIG. 4: Dependence of the strainrate and the pressure tensor components P_{xx} and P_{yy} on the range of Lucy’s weighting function $w(r < h)$ for the stationary shockwave shown in Figure 1 (but with a system width eight times larger than that of Figure 1). The widths of the curves in the Figure increase with increasing h .

two dimensions) with their orientations constrained, then the temperatures T_{xx} and T_{yy} can be independently distinguished.

The equilibrium velocity distributions, in the thermometer, are Maxwell-Boltzmann distributions. Kinetic theory shows¹⁸ that such an ideal-gas thermometer transfers energy to/from a degree of freedom if the kinetic energy of that degree of freedom is less/greater than kT_{gas} . When this simple mechanical definition of temperature is used to analyze shock-wave structure cause-and-effect relaxation and thermal anisotropy are revealed. Both these novel features need to be tackled and described by any realistic and comprehensive shock-wave model.

III. LOCAL AVERAGES AND THEIR MEASUREMENT

The temperature measurements just discussed require choosing a velocity for the thermometer. It must be *comoving* with the material in order to measure fluctuations. But exactly what is the velocity about which the fluctuations are measured? A useful answer can be found based on the weight functions used in smooth particle applied mechanics, “SPAM”^{19,20}. Lucy suggested that averages, at a fixed point in space, be computed using a

weight function $w(r < h)$ centered there, with an arbitrary width h , and normalized, so that the integral of $w(r)$ over all space is unity. The simplest weight function is a polynomial chosen so that it has a smooth maximum at the origin, $r = 0$, and two continuous derivatives everywhere. These requirements guarantee that averages computed with the weight function,

$$\langle F(r) \rangle \equiv \sum_j w_{rj} F_j / \sum_j w_{rj} ; w_{rj} \equiv w(|r - r_j|) ,$$

where $F(r)$ is a “field variable” like density, velocity, temperature, or stress, have also two continuous spatial derivatives. In the sums over nearby particles $\{j\}$ it is usual to choose the range h so that several dozen particles are included.

These conditions on the weight function are sufficient to determine its functional form:

$$w_{Lucy}(r < h) \propto [1 - 6(r/h)^2 + 8(r/h)^3 - 3(r/h)^4] .$$

Hardy’s approach²¹ to defining averages in shockwaves uses the same idea as Lucy’s. Evidently h must be large enough to avoid wiggles in the resulting averages, while remaining sufficiently small for averages to be local and inexpensive to compute. In shockwaves a value for h of about three times the interparticle spacing is a good choice. Figure 4 shows explicitly the dependence of the pressure tensor and the velocity gradient averages on the range of the weight function.

When constructing continuum models designed to reproduce atomistic simulations it is essential to specify the spatial averaging technique. The fact that the resulting constitutive equation depends on h is simply a reminder that atomistic mechanics and continuum mechanics, though similar, are not the same.

IV. EMPIRICAL RELAXATION MODELS FOR STRESS AND HEAT FLUX

A. Maxwell’s Stress Relaxation Model and its Extension to Heat Flux

Maxwell modeled the stress relaxation characteristic of viscoelastic fluids by introducing a stress relaxation time τ_σ :

$$\sigma + \tau_\sigma \dot{\sigma} = \eta \dot{\epsilon} .$$

In the shockwave problem η is the shear viscosity and $\dot{\epsilon}$ is the strainrate, (du/dx) . Both time derivatives, indicated by the superior dots, are comoving with the fluid. In the ab-

sence of relaxation, $\tau_\sigma = 0$, Maxwell's fluid model reduces to the usual Newtonian viscous incompressible fluid, with shear stress σ proportional to the instantaneous value of $\dot{\epsilon}$. In the absence of any imposed strainrate ($\dot{\epsilon} = 0$) the initial stress decays with a characteristic relaxation time τ_σ . For a delta-function strain rate, at $t = 0$, the stress has decays exponentially from its initial value:

$$\dot{\epsilon} = \delta(t = 0) \longrightarrow \sigma = (\eta/\tau)e^{-t/\tau} .$$

For a relatively-simple case, with $\eta = \tau = 1$, and a localized strain rate, like that in the Landau-Lifshitz description of a weak shock²:

$$\dot{\epsilon} = \frac{1}{e^{-t} + e^{+t}} ,$$

Maxwell's model has an analytic solution:

$$\sigma(t) = e^{-t} \ln \sqrt{1 + e^{+2t}} .$$

Figure 5 illustrates the stress response for the Newtonian case $\tau = 0$, and for two Maxwellian relaxation times, $\tau_\sigma = 1$ and $\tau_\sigma = 4$. Recent molecular dynamics shockwave simulations have shown that both stress and heat flux exhibit delayed responses⁹.

Exactly the same ideas can be, and have been²⁵, applied to heat flux. If we introduce the relaxation time τ_Q into Fourier's law for heat flow, the result is the Cattaneo equation:

$$Q + \tau_Q \dot{Q} = -\kappa \nabla T ,$$

and the heat flux lags behind the temperature gradient by a time of the order of τ .

On physical grounds the time derivative here is again comoving with the fluid. The Cattaneo equation describes heat flux and predicts its decay, just as did Maxwell's formulation of stress decay:

$$\nabla T \propto \frac{1}{e^{-t} + e^{+t}} \longrightarrow Q(t) \propto -e^{-t} \ln \sqrt{1 + e^{+2t}} .$$

In the following Section we illustrate how to incorporate these relaxation effects for stress and heat flux into a simple dense-fluid shockwave model.

B. Krook-Boltzmann Thermal Relaxation

The Boltzmann equation¹² models the dynamics of a dilute gas in which the gas particles undergo occasional two-body collisions. The evolution of the velocity distribution function,

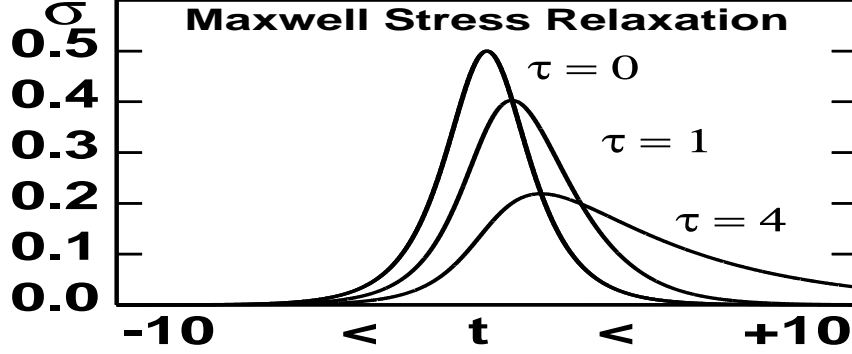


FIG. 5: Delayed stress σ in response to the strain rate $1/[e^{-t} + e^{+t}]$ with unit viscosity, $\eta = 1$. Maxwell’s relaxation time τ controls the stress response: $\sigma + \tau\dot{\sigma} = \eta\dot{\epsilon}$.

$f(p, r, t)$ for the phase-space density of particles with momentum p at location r at time t , can be approximated by an exponential relaxation toward equilibrium:

$$(df/dt) \equiv [f_{eq} - f]/\tau \longleftrightarrow f + \tau(df/dt) = f_{eq} .$$

This approximate “Krook-Boltzmann” equation has exactly the same form as do the Maxwell and Cattaneo relaxation equations. Here the relaxation time τ defined by this approximate equation is of the order of the mean collision time. Because two-body “conservative” collisions conserve mass, momentum, and energy, the equilibrium distribution, toward which f relaxes, necessarily has the same density, stream velocity, and energy, as does the nonequilibrium distribution f .

Shockwaves convert macroscopic longitudinal kinetic energy into microscopic “thermal” internal energy,

$$\Delta u^2/2 \longrightarrow \Delta e ,$$

through collisions, so that it is reasonable to expect shockwave stresses and temperatures to relax and equilibrate in a time of order the collision time τ . We include these delay and relaxation effects in the macroscopic model formulated in the next Section.

V. FORMULATION OF A MACROSCOPIC MODEL

Any solution of the continuum evolution equations,

$$\dot{\rho} = -\rho \nabla \cdot u ; \rho \dot{u} = -\nabla \cdot P ; \rho \dot{e} = -\nabla u : P - \nabla \cdot Q ,$$

requires constitutive models giving the pressure tensor P and heat flux Q in terms of the underlying variables $\{ \rho, u, e \}$, the density, velocity, and energy per unit mass. For completeness, in view of the relaxational results from molecular dynamics simulations, we must include separate tensor temperature components, T_{xx} and T_{yy} , in the list of state variables. In a gas the difference is simply related to the pressure tensor:

$$(T_{xx} - T_{yy}) = (P_{xx} - P_{yy})/(\rho k) ,$$

where k is Boltzmann's constant per unit mass.

In a dense fluid, the potential contribution to anisotropy is comparable to the kinetic contribution²⁶. A semiquantitative description of the potential part of the shear stress results if the equilibrium fluid structure is sheared, at the strainrate $\dot{\epsilon}$, for the Maxwell relaxation time τ_σ . The shear distortion of the pair distribution function in dense fluids has been studied experimentally²⁷ and modeled with molecular dynamics²⁶. In both cases Maxwell's relaxation provides a good description of the potential contribution to the shear stress. Thus the gas-phase description of shear anisotropy must be modified in order to describe dense fluids.

To solve this problem we choose to separate the work and heat contributing to energy change into separate longitudinal and transverse parts. The simplest choice is a time-independent division of work and heat into longitudinal and transverse parts:

$$\begin{aligned} -\alpha \nabla u : P &\longrightarrow \Delta T_{xx} ; & -(1 - \alpha) \nabla u : P &\longrightarrow \Delta T_{yy} ; \\ -\beta \nabla \cdot Q &\longrightarrow \Delta T_{xx} ; & -(1 - \beta) \nabla \cdot Q &\longrightarrow \Delta T_{yy} . \end{aligned}$$

The Navier-Stokes equations correspond to the choice $\alpha = \beta = 1/2$. In a shockwave, where the kinetic energy is initially longitudinal, we would expect instead $\alpha \simeq \beta \simeq 1$.

To explore the consequences of this division we consider in what follows a simple van der Waals model, with the energy and equilibrium pressure expressed as sums of density-dependent and temperature-dependent contributions. A slightly more flexible model⁸ can

be based on Grüneisen’s separation of the energy and pressure into corresponding “cold” and “thermal” parts.

Away from equilibrium we include Maxwell’s delayed viscous response in the pressure tensor. For a two-dimensional fluid undergoing uniaxial compression and with shear viscosity η and vanishing bulk viscosity, we have:

$$P_{xx} = P_{\text{eq}} - \sigma ; P_{yy} = P_{\text{eq}} + \sigma ; \sigma + \tau_{\sigma}\dot{\sigma} = \eta(du/dx) .$$

The stress relaxation time τ_{σ} describes the delay in the response of the shear stress σ to the strainrate $\dot{\epsilon} = (du/dx)$.

If the longitudinal and transverse temperatures are constrained to differ, we would expect the stationary nonequilibrium heat flux vector to obey a tensor form of Fourier’s law:

$$Q_x = -\kappa_{xx}(dT_{xx}/dx) - \kappa_{yy}(dT_{yy}/dx) .$$

In the shockwave problem the effects of delay and eventual equilibration both need to be included. For simplicity we add on corresponding delays and thermal relaxation to the continuum evolution equations for the heat flux and the temperatures:

$$\dot{Q}_x \supset -Q_x/\tau_Q ; \dot{T}_{xx} \supset (T_{yy} - T_{xx})/\tau_T ; \dot{T}_{yy} \supset (T_{xx} - T_{yy})/\tau_T .$$

To model a dense N -particle van der Waals fluid, as opposed to a dilute gas, we approximate the potential part of the thermal energy by setting it equal to the kinetic part:

$$E_{\Phi} - E_{\text{Cold}} \simeq E_K = Nk(T_{xx} + T_{yy})/2 \longrightarrow E_{\text{Thermal}} = Nk(T_{xx} + T_{yy}) .$$

The motivation for studying such simple continuum models derives from the results of molecular dynamics simulations of stationary shockwaves⁸⁻¹⁰. Just as in the continuum case, these microscopic molecular dynamics simulations conserve mass, momentum, and energy, so that the stationary fluxes of these quantities,

$$\rho u , P_{xx} + \rho u^2 ; \rho u[e + (P_{xx}/\rho) + (u^2/2)] + Q_x ,$$

are constant throughout the flow. These simulations show further that both the stress and heat flux lag behind the strainrate and temperature gradient. The lags are physically reasonable from the collisional cause-and-effect standpoint.

Newton’s viscosity and Fourier’s heat conduction both describe *instantaneous* relationships. Taken literally, these two linear laws imply that the stress σ and heat flux Q respond instantaneously, and supersonically, to the strainrate $\dot{\epsilon}$ and temperature gradient ∇T .

Certainly such an instantaneous response is impossible. If we imagine reversing a time-reversible Newtonian motion of the shock process, another apparent shortcoming of the Navier-Stokes formulation is revealed. Newton’s and Fourier’s laws,

$$\sigma \propto \dot{\epsilon} ; Q_x \propto -(dT/dx) ,$$

if applied to a time-reversible flow, imply that the stress changes sign (as $\dot{\epsilon}$ changes sign when the motion is reversed) while the heat flux does not (as the temperature gradient has no time-dependence). Both conclusions are inconsistent with time-reversible Newtonian dynamics.

A detailed atomistic analysis of the pressure tensor and the heat flux vector²⁴ shows that these functions are respectively even and odd functions of time, so that Newton’s and Fourier’s ideas are necessarily inexact as they lack the proper delay time inherent in inter-particle collisions. Lacking a more fundamental approach to time-reversible irreversibility, we seek to learn more by exploring explicitly the irreversible nature of continuum models.

VI. NUMERICAL SOLUTIONS OF THE VAN DER WAALS SHOCKWAVE MODEL

A one-dimensional “staggered grid”, with density evaluated within N_c cells of length dx , bounded by $N_n = N_c + 1$ nodes, and with the remaining long list of time-dependent variables $\{u, e, T_{xx}, T_{yy}, \sigma, Q\}$ given at the nodes, provides a basis for an iterative solution of the continuum equations^{10,28}. Our assumption relating the energy change to the changes in the two temperatures gives the set of nodal variables $\{u, T_{xx}, T_{yy}, \sigma, Q\}$ with the internal energy density given by

$$e \equiv (\rho/2) + kT_{xx} + kT_{yy} .$$

We have found that such an approach can be applied to wave-structure relaxation with longitudinal and transverse work and heat separation, as well. The Landau-Lifshitz weak-shock solution² – for constant shear viscosity and thermal conductivity, and without any relaxation – makes a useful initial condition. In the stationary-shockwave coordinate system

Work & Heat Both Initially Longitudinal

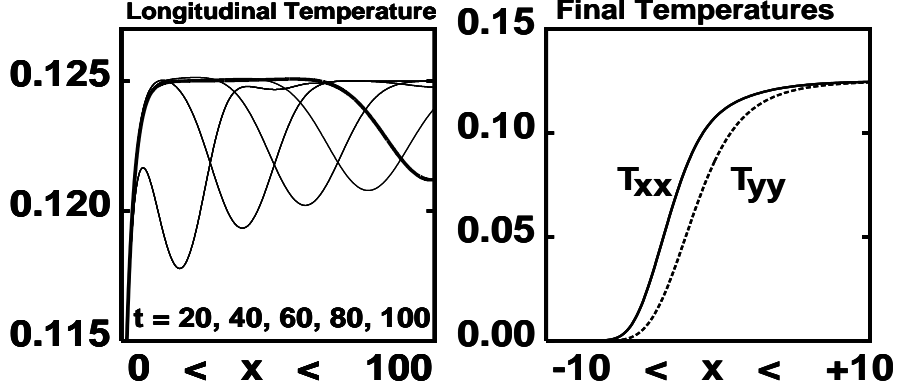


FIG. 6: Development of the stationary temperature profiles in a shockwave with shear viscosity ($\eta = 4$), heat conductivities $\{\kappa_{xx} = \kappa_{yy} = 2\}$ and relaxation times $\{\tau_{\sigma} = \tau_Q = \tau_r = 1\}$. The converged temperatures are shown at the right. Here the work done and the heat transfer initially affect only the longitudinal temperature.

errors in the initial condition move to the right, away from the shockwave, at approximately the speed of sound. See Figures 6 and 7 for transient results from typical solutions of the continuum equations..

A successful numerical evolution algorithm proceeds from an initial guess by iterating a series of four steps: (i) specify the six dependent variables $\{\rho_c, v_n, T_{xxn}, T_{yy n}, \sigma_n, Q_n\}$ at all the interior cells and nodes; (ii) compute all the remaining variables and all the gradients with centered sums and differences:

$$u_c(x) = [u_n(x - dx/2) + u_n(x + dx/2)]/2 ; \rho_n(x) = [\rho_c(x - dx/2) + \rho_c(x + dx/2)]/2 ;$$

$$dT_{ii}/dx = [T_{ii}(x + dx/2) - T_{ii}(x - dx/2)]/dx ;$$

(iii) compute the righthandsides of the five sets of differential equations.

For instance, the change in energy at a particular node could be evaluated as follows:

$$(\partial e/\partial t)_n = -u_n(de/dx)_n - [(P_{xx}du/dx)_n + (dQ_x/dx)_n]/\rho_n ;$$

(iv) use the fourth-order Runge-Kutta method to integrate the $N_c + 5N_n$ ordinary differential equations for one timestep dt , providing the information necessary for a return to step (i) for the execution of the next timestep. The numerical values of the mass, momentum, and

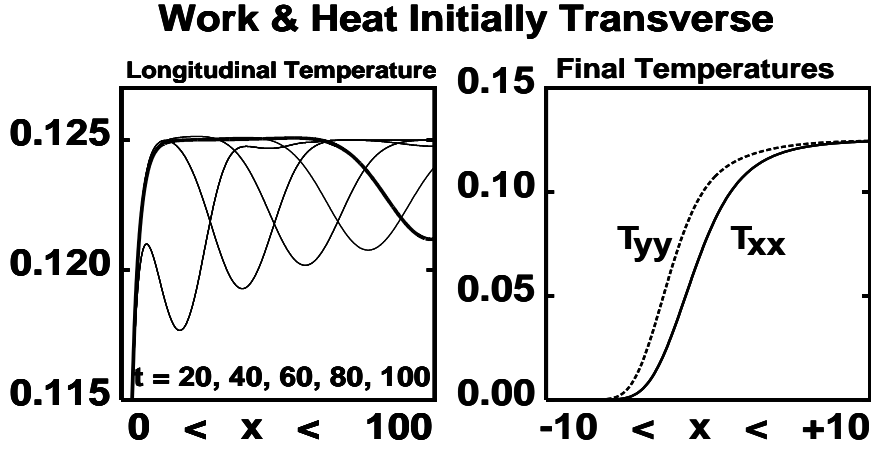


FIG. 7: Development of the stationary temperature profiles in a shockwave with shear viscosity ($\eta = 4$), heat conductivities $\{\kappa_{xx} = \kappa_{yy} = 2\}$ and relaxation times $\{\tau_\sigma = \tau_Q = \tau_r = 1\}$. The converged temperatures are shown at the right. Here the work done and the heat transfer initially affect only the transverse temperature.

energy, as well as their fluxes can be used to help estimate the initial conditions. For the twofold compression shockwave we use to illustrate these ideas, the fluxes and boundary values are the following:

$$\begin{aligned}
 P_{eq} &= \rho e ; e = (\rho/2) + T_{xx} + T_{yy} ; e_{eq} = (\rho/2) + 2T ; \\
 \rho u &= 2 ; P_{xx} + \rho u^2 = 9/2 ; (\rho u)[e + (P_{xx}/\rho) + (u^2/2)] + Q_x = 6 ; \\
 \rho : (2 \rightarrow 1) ; u : (1 \rightarrow 2) ; P : (1/2 \rightarrow 5/2) ; T : (0 \rightarrow 1/8) ; e : (1/2 \rightarrow 5/4) .
 \end{aligned}$$

Here the cold and hot boundary values are linked by arrows: (*cold* \rightarrow *hot*). Both Q_x and σ necessarily vanish at the boundaries, $Q_x : (0 \rightarrow 0)$; $\sigma : (0 \rightarrow 0)$.

Figures 6, 7, and 8 illustrate typical solutions. In order to circumvent numerical instabilities in the numerical work one can (i) increase the number of cells, (ii) reduce the timestep and/or cell size, (iii) introduce an explicit artificial time-dependence in the parameters $\{\eta, \kappa, \tau\}$ in order to enhance convergence. In this way we have obtained solutions of the continuum shockwave model for a wide range of parameters. The same ideas can be used to study special cases in which stress or heat flux are not delayed or in which temperature is scalar rather than tensor. The sample solutions shown in Figures 6-8 show how the partition of heat and work can affect the stationary shockwave.

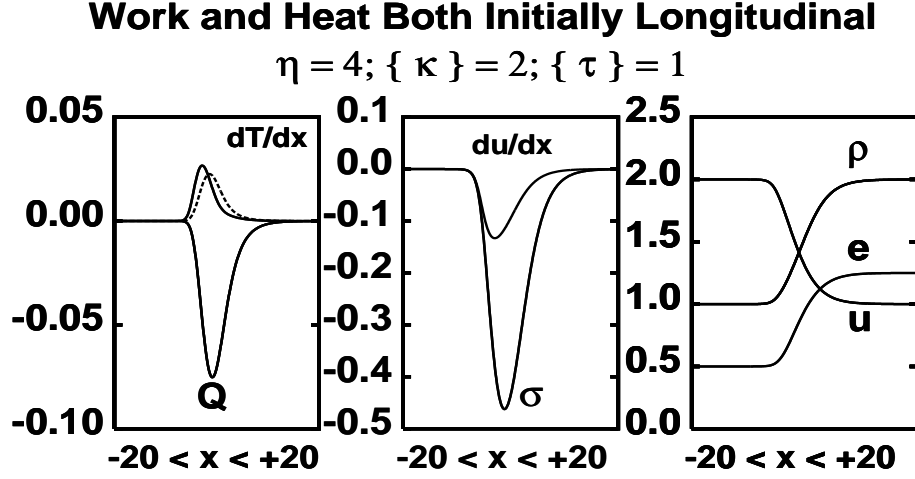


FIG. 8: Stationary profiles showing the longitudinal and transverse temperature gradients [(dT_{xx}/dx) is solid; (dT_{yy}/dx) is dashed] as well as the velocity gradients. Notice that the heat flux and shear stress lag behind the gradients which “cause” them.

VII. CONCLUSIONS AND PROSPECTS

The simulation of nonequilibrium stationary states with molecular dynamics, particularly in the two-block geometry of Figure 2, emphasizes Loschmidt’s reversibility paradox^{12,24,29,30}. Evidently a movie of exactly the same dynamical states, played backward in time, satisfies all the microscopic motion equations. Such reversed motions contradict macroscopic physics and are never observed in practice. They would be inherently Lyapunov unstable, with any small perturbation (such as roundoff in the last place) growing exponentially in time and so destroying the reversed trajectory.

Because time-reversed solutions of the Newtonian equations of motion are not observable it is legitimate to use time-irreversible models in interpreting the solutions. The noticeable time-delays, for both stress and heat flux, observed in these solutions legitimates also the use of Maxwell-Cattaneo-Krook relaxation. These innovations are useful to the goal of finding macroscopic descriptions conforming to microscopic observations.

Although we have been able to find stable solutions for the most general description considered here (three relaxation times, partition of heat and work, tensor temperature) there are stringent limits on the parameter ranges for which such solutions exist. On physical grounds stress and heat flux relaxation must be relatively rapid. A fluid’s memory cannot be

too long. A systematic study of stability is complicated by the large number of parameters involved. Nevertheless, carefully chosen example cases should shed additional light on the physics of relaxation and of strong shockwaves. At the moment the step of generalizing the physical ideas further, for instance by considering the state dependence of the relaxation times, is premature. But we can confidently expect progress there in the future.

VIII. ACKNOWLEDGMENTS

We specially thank Brad Holian for his comments, suggestions, and prepublication copies of Reference 10. Vitaly Kuzkin provided the motivation for this work, through his invitation and support for WGH and CGH's contributions to the International Summer School-Conference "Advanced Problems in Mechanics-2010" organized by the Institute for Problems in Mechanical Engineering of the Russian Academy of Sciences in Mechanics and Engineering under the patronage of the Russian Academy of Sciences.

-
- ¹ C. E. Ragan, III, "Shockwave Experiments at Threefold Compression", *Physical Review A* **29**, 1391-1402 (1984).
 - ² L. D. Landau and E. M. Lifshitz, *Fluid Mechanics* (Pergamon, Oxford, 1959). Chapter IX is devoted to shockwaves.
 - ³ R. E. Duff, W. H. Gust, E. B. Royce, M. Ross, A. C. Mitchell, R. N Keeler, and W. G. Hoover, "Shockwave Studies in Condensed Media", in *Behavior of Dense Media under High Dynamic Pressures*, Proceedings of the 1967 Paris Conference, pages 397-406 (Gordon and Breach, New York, 1968)
 - ⁴ V. Y. Klimenko and A. N. Dremin, "Structure of Shockwave Front in a Liquid", pages 79-83 in *Detonatsiya, Chernogolovka* (Akademia Nauk, Moscow, 1978).
 - ⁵ B. L. Holian, W. G. Hoover, B. Moran, and G. K. Straub, "Shockwave Structure *via* Nonequilibrium Molecular Dynamics and Navier-Stokes Continuum Mechanics", *Physical Review A* **22**, 2798-2808 (1980).
 - ⁶ B. L. Holian, "Modeling Shockwave Deformation *via* Molecular Dynamics", *Physical Review A* **37**, 2562-2568 (1988).

- ⁷ Wm. G. Hoover and C. G. Hoover, “Tensor Temperature and Shockwave Stability in a Strong Two-dimensional Shockwave”, *Physical Review E* **80**, 011128 (2009).
- ⁸ Wm. G. Hoover and C. G. Hoover, “Well-Posed Two-Temperature Constitutive Equations for Stable Dense Fluid Shockwaves using Molecular Dynamics and Generalized Navier-Stokes-Fourier Continuum Mechanics”, *Physical Review E* **81**, 046302 (2010).
- ⁹ Wm. G. Hoover and C. G. Hoover, “Shockwaves and Local Hydrodynamics; Failure of the Navier-Stokes Equations”, in *New Trends in Statistical Physics, Festschrift in Honor of Leopoldo García-Colín’s 80th Birthday*, edited by Alfredo Macias and Leonardo Dagdug (World Scientific, Singapore, 2010).
- ¹⁰ B. L. Holian and M. Mareschal, “A New Heat-Flow Equation Motivated by the Ideal-Gas Shockwave”, (unpublished, 2009); B. L. Holian, M. Mareschal, and R. Ravelo, “Test of a New Heat-Flow Equation for Dense-Fluid Shockwaves”, *Journal of Chemical Physics* (submitted, 2010).
- ¹¹ W. G. Hoover, “Structure of a Shockwave Front in a Liquid”, *Physical Review Letters* **42**, 1531-1534 (1979).
- ¹² L. Boltzmann, *Lectures on Gas Theory*, translated by S. G. Brush (University of California Press, Berkeley, 1964).
- ¹³ H. M. Mott-Smith, “The Solution of the Boltzmann Equation for a Shockwave”, *Physical Review* **82**, 885-892 (1951).
- ¹⁴ K. Xu and E. Josyula, “Multiple Translational Temperature Model and its Shock Structure Solution”, *Physical Review E* **71**, 056308 (2005).
- ¹⁵ E. Salomons and M. Mareschal, “Usefulness of the Burnett Description of Strong Shock Waves”, *Physical Review Letters* **69**, 269-272 (1992).
- ¹⁶ F. J. Uribe, R. M. Velasco, and L. S. García-Colín, “Burnett Description of Strong Shock Waves”, *Physical Review Letters* **81**, 2044-2047 (1998).
- ¹⁷ F. J. Uribe, R. M. Velasco, L. S. García-Colín, and E. Díaz-Herrera, “Shockwave Profiles in the Burnett Approximation”, *Physical Review E* **62**, 6648-6666 (2000).
- ¹⁸ W. G. Hoover, B. L. Holian, and H. A. Posch, “Comment I on ‘Possible Experiment to Check the Reality of a Nonequilibrium Temperature’”, *Physical Review E* **48**, 3196-3198 (1993).
- ¹⁹ L. B. Lucy, “A Numerical Approach to the Testing of the Fission Hypothesis”, *The Astronomical Journal* **82**, 1013-1024 (1977).

- ²⁰ Wm. G. Hoover, *Smooth Particle Applied Mechanics; the State of the Art* (World Scientific, Singapore, 2006).
- ²¹ R. J. Hardy, “Formulas for Determining Local Properties in Molecular-Dynamics Simulations: Shockwaves”, *Journal of Chemical Physics* **76**, 622-628 (1982).
- ²² D. Gilbarg and D. Paolucci, “The Structure of Shockwaves in the Continuum Theory of Fluids”, *Journal of Rational Mechanics Analysis* **2**, 617-642 (1953).
- ²³ B. L. Holian, C. W. Patterson, M. Mareschal, and E. Salomons, “Modeling Shockwaves in an Ideal Gas: Going Beyond the Navier-Stokes Level”, *Physical Review E* **47**, R24-R27 (1993).
- ²⁴ Wm. G. Hoover, *Computational Statistical Mechanics* (Elsevier, Amsterdam, 1991, available without charge at <http://williamhoover.info/book.pdf>).
- ²⁵ D. D. Joseph and L. Preziosi, “Heat Waves”, *Reviews of Modern Physics* **61**, 41-73 (1989) with an Addendum in *Reviews of Modern Physics* **62**, 375-391 (1990).
- ²⁶ W. T. Ashurst and W. G. Hoover, “Dense-Fluid Shear Viscosity *via* Nonequilibrium Molecular Dynamics”, *Physical Review A* **11**, 658-678 (1975). See Figure 6.
- ²⁷ N. A. Clark and B. J. Ackerson, “Observation of the Coupling of Concentration Fluctuations to Steady-State Shear Flow”, *Physical Review Letters* **44**, 1005-1008 (1980).
- ²⁸ A. Puhl, M. M. Mansour, and M. Mareschal, “Quantitative Comparison of Molecular Dynamics with Hydrodynamics in Rayleigh-Bénard Convection”, *Physical Review A* **40**, 1999-2012 (1989).
- ²⁹ B. L. Holian, W. G. Hoover, and H. A. Posch, “Resolution of Loschmidt’s Paradox: The Origin of Irreversible Behavior in Reversible Atomistic Dynamics”, *Physical Review Letters* **59**, 10-13 (1987).
- ³⁰ Wm. G. Hoover, *Time Reversibility, Computer Simulation, and Chaos* (World Scientific, Singapore, 2001).